Curing Kinetics and Thermal Property Characterization of an *o*-Cresol Formaldehyde Epoxy Resin and 4,4′-Diaminodiphenyl Ether System

Jungang Gao, Min Zhao

Department of Chemistry and Environmental Science, Hebei University, Baoding 071002, People's Republic of China

Received 24 November 2003; accepted 30 March 2004
DOI 10.1002/app.20853
Published online in Wiley InterScience (www.interscience.wiley.com).

ABSTRACT: The kinetics of the curing reaction for a system of *o*-cresol formaldehyde epoxy resin (*o*-CFER) with 4,4′-diaminodiphenyl ether (DDE) as a curing agent were investigated with differential scanning calorimetry (DSC). An analysis of the DSC data indicated that an autocatalytic behavior appeared in the first stages of the cure for the system, and this could be well described by the model proposed by Kamal, which includes two rate constants and two reaction orders (m and n). The overall reaction order ($m + n$) was 2.7–3.1, and the activation energies were 66.79 and 49.29 kJ mol^{-1}, respectively. In the later stages, a crosslinked network was formed, and the reaction was mainly controlled by diffusion. For a more precise consideration of the diffusion effect, a diffusion factor was added to Kamal's equation. In this way, the curing kinetics were predicted well over the entire range of conversions, covering both the previtrification and postvitrification stages. The glass-transition temperatures of the *o*-CFER/DDE samples were determined via torsional braid analysis. The results showed that the glass-transition temperatures increased with the curing temperature and conversion up to a constant value of approximately 370 K. The thermal degradation kinetics of the system were investigated with thermogravimetric analysis, which revealed two decomposition steps. © 2004 Wiley Periodicals, Inc. J Appl Polym Sci 94: 182–188, 2004

Key words: resins; thermal properties; kinetics; glass transition

INTRODUCTION

Epoxy resins are widely used in the polymer industry as coatings, structural adhesives, insulating materials, polymer matrices for composite materials, and so forth. The widespread use of epoxy resins, however, is limited in many high-performance applications because of their thermal properties. The factors that most influence the thermal properties of epoxy resins are the crosslink density and the structure of the molecular chain. With the addition of *o*-cresol groups to the backbone of epoxy resins, the improved resins are considered worthy of further study in terms of their good thermal stability, chemical resistance, mechanical properties, and modification.[1,2]

Studies of the applications and physical properties of *o*-cresol formaldehyde epoxy resin (*o*-CFER) have been reported extensively in recent years.[3,4] However, descriptions of the cure kinetics and degradation kinetics of *o*-CFER with 4,4′-diaminodiphenyl ether (DDE) have been lacking until now.

To provide a basis for curing process theory for applications of *o*-CFER, we must conduct research into the curing kinetics of the *o*-CFER/DDE system. Kamal's model,[5] arising from an autocatalytic reaction mechanism, has been applied to isothermal differential scanning calorimetry (DSC) data.[6–8] In general, a good fit of the experimental data has been obtained for the early stages of the cure, but deviations have been observed in the later stages, particularly near vitrification when the reaction is primarily diffusion-controlled. For the consideration of the diffusion effect, the Kamal model has been extended by the addition of a diffusion factor [$f(\alpha)$].

In this study, DSC was used to study the curing kinetics of *o*-CFER/DDE. Because the glass-transition temperature (T_g) could be used effectively to monitor the curing reaction,[9] torsional braid analysis (TBA) was used to determine T_g of the *o*-CFER/DDE system. The T_g's were measured for *o*-CFER/DDE samples cured isothermally at different temperatures for various periods. Structural changes during the curing process were investigated with Fourier transform infrared (FTIR). The mechanism of thermal degradation was studied with thermogravimetric analysis (TGA). TGA data were analyzed according to the literature.[10,11]

EXPERIMENTAL

Materials

Epichlorohydrin, *o*-cresol, formaldehyde, NaOH, KOH, acetone, ethyl alcohol, hydrochloric acid, and

Correspondence to: J. Gao (gaojg@mail.hbu.edu.cn).

DDE were all analytically pure and were supplied by Beijing Chemical Reagent Co. (Beijing, China).

Synthesis of *o*-CFER

An epoxy resin based on *o*-cresol formaldehyde (*o*-CFER) was synthesized according to the literature.[12] The molecular structure of this resin was as follows:

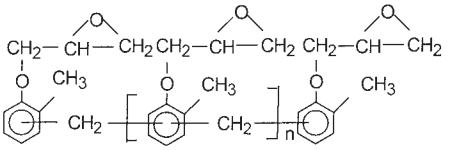

where n was 0–1. The epoxy value was determined with Jay's method[13] to be 0.312 mol/100 g.

IR measurements

The *o*-CFER/DDE samples were prepared with a stoichiometric ratio of one epoxy group to one *N*-hydrogen. During the isothermal curing, an FTS-40 IR spectrophotometer (Bio-Rad Co., Ltd., USA) was used for the investigation of the structural changes of the curing system. The sample was dissolved in acetone and then coated as a thin film on a potassium bromide plate. Afterwards, the plate was placed in a heated oven at a fixed temperature of 423 K. During the curing reaction at this temperature, the plate was repeatedly scanned at a regular time interval for analysis.

DSC method

Curing studies were carried out on a DT-41 differential scanning calorimeter (Shimadzu Co., Ltd., Japan). The DSC instrument was calibrated with high-purity indium; α-Al_2O_3 was used as the reference material. Isothermal and dynamic heating experiments were carried out according to the methods of Opalicki et al.[6] under a nitrogen flow of 40 mL min^{-1}.

o-CFER and the hardener DDE were mixed homogeneously in a 1:1 molar ratio of active hydrogens to epoxy groups. The samples (ca. 10 mg) of the mixture were weighed accurately into an aluminum DSC sample pan, which was sealed with an aluminum lid. The entire operation was carried out in a dry chamber. The samples were placed in thermostatic baths at curing temperatures (T_c's) of 403, 413, 418, and 423 K. The reaction was considered complete when the rate curve leveled off to the baseline. The total area under the exothermal curve, based on the extrapolated baseline at the end of the reaction, was used to calculate the isothermal heat of cure (ΔH_i) at a given temperature. After each isothermal run, the sample was quenched to 283 K and then reheated at 10 K min^{-1} to 573 K to determine the residual heat of reaction (ΔH_r). The total heat that evolved during the curing reaction was $\Delta H_0 = \Delta H_i + \Delta H_r$.

TBA

The specimens were prepared via the dipping of heat-cleaned glass fiber braid into an acetone solution of the *o*-CFER/DDE system at a 1:1 molar ratio, and then the acetone was completely evaporated *in vacuo*. The air oven was first heated up to the desired T_c and kept there for a certain period until the system reached the equilibrium state. The specimens were quickly set into the thermostatic baths at T_c's of 403, 413, 418, and 423 K for 15, 30, 60, 90, 120, 180, and 240 min. Then, they were taken out and cooled to room temperature, and their T_g's were determined with TBA at a heating rate of 2 K min^{-1}.

TGA

o-CFER and DDE were mixed in a 1:1 molar ratio. After 600 min of curing at 423 K, the thermal analysis was carried out on a Shimadzu DT-40 thermogravimetric analyzer under a static air atmosphere. About 3 mg of a sample, which had been completely cured, was placed in a platinum cell and placed on the detector plate, and then the furnace was heated to 923 K at a heating rate of 10 K min^{-1}.

RESULTS AND DISCUSSION

Isothermal curing

FTIR spectra of the *o*-CFER/DDE system are shown in Figure 1. The most significant feature is the epoxide group absorption at 914 cm^{-1} (marked by an arrow). This absorption peak of *o*-CFER/DDE cured for 600 min at 423 K is much lower than that of noncured *o*-CFER. In addition, the IR absorption in the carbonyl region practically did not change.

The mechanisms of the curing reaction of thermosetting resins have two general kinetic models: *n*th-order kinetics and autocatalytic kinetics.[10] The reaction rate of *n*th-order kinetics can be expressed as follows:

$$\frac{d\alpha}{dt} = K(T)(1 - \alpha)^n \quad (1)$$

The reaction rate of autocatalytic kinetics can be defined as follows:

$$\frac{d\alpha}{dt} = k'\alpha^m(1 - \alpha)^n \quad (2)$$

where α is the extent of the reaction or conversion ($\alpha = \Delta H_t/\Delta H_0$, where ΔH_t is the partial area under a DSC

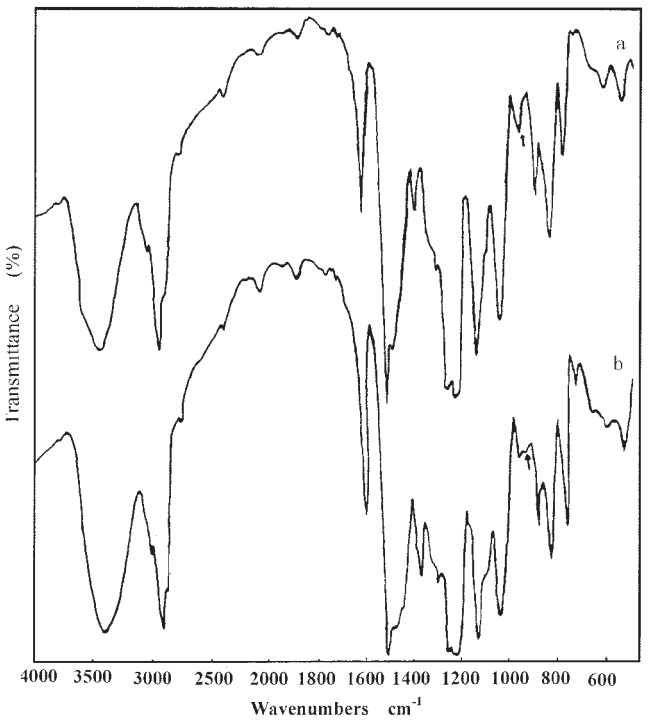

Figure 1 FTIR spectra of *o*-CFER/DDE after curing at 423 K for (a) noncured *o*-CFER and (b) *o*-CFER cured for 600 min.

trace up to time t), m and n are the reaction orders, and k' is the kinetic rate constant.

To consider the autocatalytic reaction, for which the initial reaction rate of the autocatalytic reaction is not zero, Kamal[5] proposed the following generalized expression:

$$\frac{d\alpha}{dt} = (k_1 + k_2\alpha^m)(1 - \alpha)^n \tag{3}$$

where $k_1$and k_2 are the specific rate constants, which are functions of the temperature. According to the nth-order kinetic model, the maximum reaction rate is observed at $t = 0$, and according to the autocatalytic model, the reaction rate is zero initially and attains the maximum value at some intermediate conversion.

During the curing reaction of thermosetting resins, the heat evolution recorded by DSC is proportional to the extent of consumption of the epoxide groups in the epoxy resins or the reactive groups in the curing agent;[14,15] that is, the released heat is proportional to the extent of the reaction. Following this assumption, we studied the curing kinetics and determined the kinetic data.[16,17] If the cure reaction is the only thermal event, then the reaction rate ($d\alpha/dt$) is proportional to the heat flow (dH/dt):[10]

$$\frac{d\alpha}{dt} = \frac{dH/dt}{\Delta H_0} \tag{4}$$

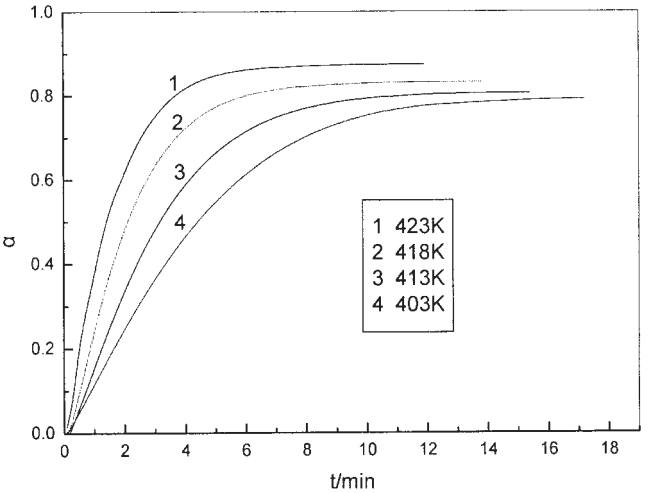

Figure 2 α versus time t at different T_c's.

The rate of cure can be determined with the curing exotherm.

Figure 2 shows plots of α versus time t at different isothermal temperatures, and isothermal DSC curves of $d\alpha/dt$ versus time t are shown in Figure 3. The reaction rate at any temperature increased with time during the initial stage of cure and passed through a maximum. The peak of the reaction rate became higher and shifted to a shorter time with increasing T_c. However, α reached only about 80–90% in the time of the experiment. The plots show a maximum reaction rate at time $t > 0$, and this negates simple nth-order kinetics. For the computation of the kinetic parameters in eq. (3), several methods have been proposed.[18–20] In this study, k_1 was graphically calculated as the initial reaction rate at time $t = 0$, given by the intercept of Figure 3. Then, k_2, m, and n were calculated through nonlinear regression according to eq. (3). The resulting data are shown in Table I. $m + n$ is the overall reaction order.

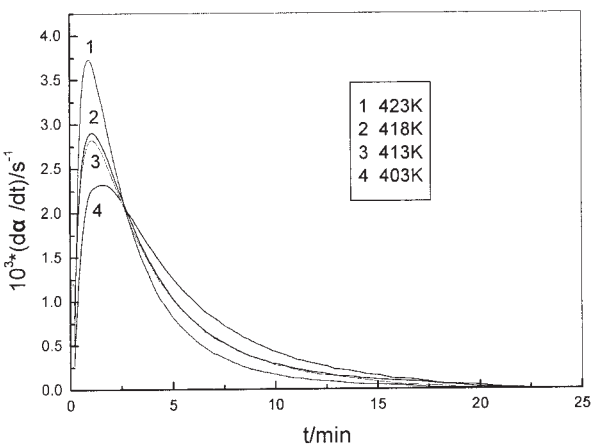

Figure 3 $d\alpha/dt$ versus t at different temperatures.

TABLE I
Kinetic Parameters for the Isothermal Curing of *o*-CFER/DDE

Temperature (K)	403	413	418	423
k_1 ($\times 10^{-3}$ s^{-1})	0.979	1.69	1.96	2.46
k_2 ($\times 10^{-3}$ s^{-1})	5.49	8.06	9.08	11.7
m	0.58	0.64	0.73	0.64
n	2.18	2.28	2.31	2.39
$m + n$	2.76	2.92	3.04	3.03

Table I shows that the k_1 values were small in comparison with k_2, which affected the reaction more. Furthermore, k_1 and k_2 increased with T_c. The overall reaction order, $m + n$, was 2.7–3.1. k_1 and k_2 depended on the temperature and followed an Arrhenius relationship:

$$k_i = A_i \exp(-E_i/RT) \quad i = 1, 2 \tag{5}$$

where A_i is the pre-exponential constant, E_i is the activation energy, R is the gas constant, and T is the absolute temperature. k_1 and k_2 are shown in an Arrhenius plot in Figure 4; the associated activation energies E_1 and E_2 were 66.89 and 49.29 kJ/mol, respectively. The linear correlation coefficient was 0.9948 for k_1 and 0.9969 for k_2.

Typical comparisons between the experimental DSC data for two temperatures (413 and 423 K) and the autocatalytic model with parameters from eq. (3) are shown in Figure 5. The kinetic behavior described by the kinetic model agrees with the experimental data in the early stage. As the reaction progresses, a deviation appears because of the onset of gelation and vitrification, but the mobility of reactive groups is hindered, and the rate of conversion is controlled by diffusion rather than by kinetic factors.[21] Differences between

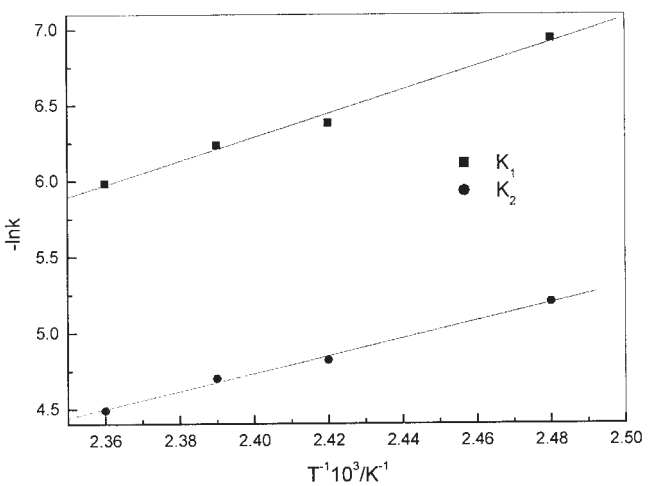

Figure 4 k_1 and k_2 versus temperature T.

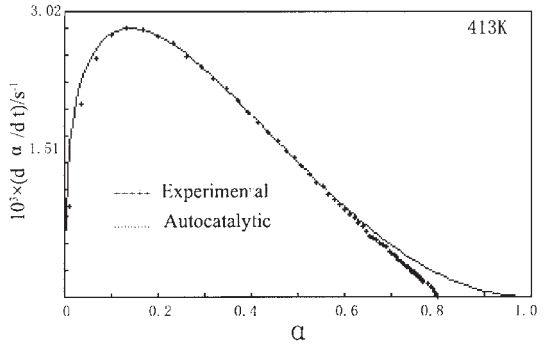

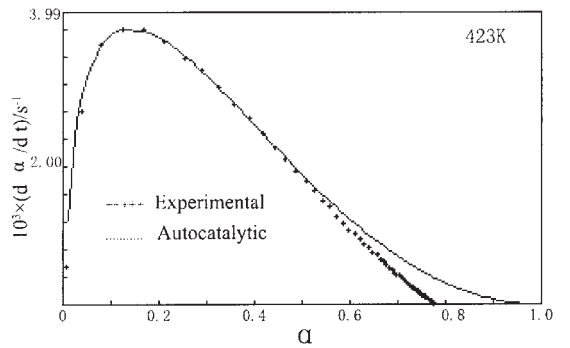

Figure 5 Comparison of the experimental data and theoretical values: $d\alpha/dt$ versus α at 413 and 423 K

the model predictions and experimental data were observed. They could be interpreted in terms of free-volume considerations.[22] The free volume of materials decreases with the temperature, and then the rate of diffusion of reactive groups is reduced; this leads to a decreasing reaction rate.

To consider the diffusion effect more precisely, Cole et al.[21] proposed a semiempirical relationship based on free-volume considerations and earlier work by Chern and Poehlein.[22] In this relationship, $f(\alpha)$ is defined with two empirical parameters as follows:

$$f(\alpha) = \frac{1}{1 + \exp[C(\alpha - \alpha_c)]} \tag{6}$$

where C is the diffusion coefficient and α_c is the critical conversion depending on T_c. Plots of $f(\alpha)$ versus α at different T_c's are shown in Figure 6. For $\alpha \ll \alpha_c$, $f(\alpha)$ approximately equals unity, and the effect of diffusion is negligible; therefore, the reaction is kinetically controlled. As α approaches α_c, $f(\alpha)$ begins to decrease, reaching a value of 0.5 at $\alpha = \alpha_c$. Beyond that point, it continues to decrease and approaches zero, and this means that the reaction becomes very slow and effectively stops.

In light of the diffusion effect, the reaction rate of cure can be expressed in the following form to account for the effects of diffusion:

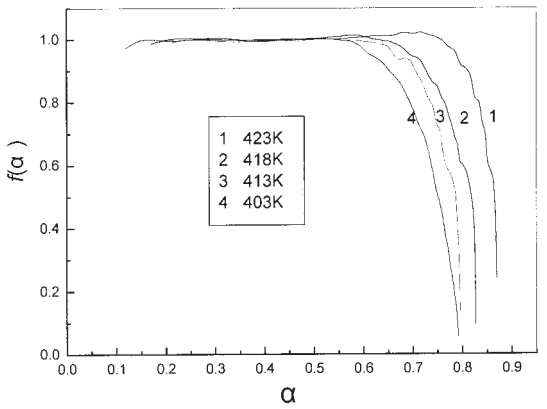

Figure 6 $f(\alpha)$ versus α at different T_c's.

$$\frac{d\alpha}{dt} = (k_1 + k_2\alpha^m)(1-\alpha)^n \frac{1}{1+\exp[C(\alpha-\alpha_c)]} \quad (7)$$

Figure 7 presents the experimental values and those obtained from eq. (7). The calculated values agree very well with the experimental data. Therefore, we employ the proposed generalized kinetic model to predict and describe the advance of our epoxy resin systems as a function of T_c.

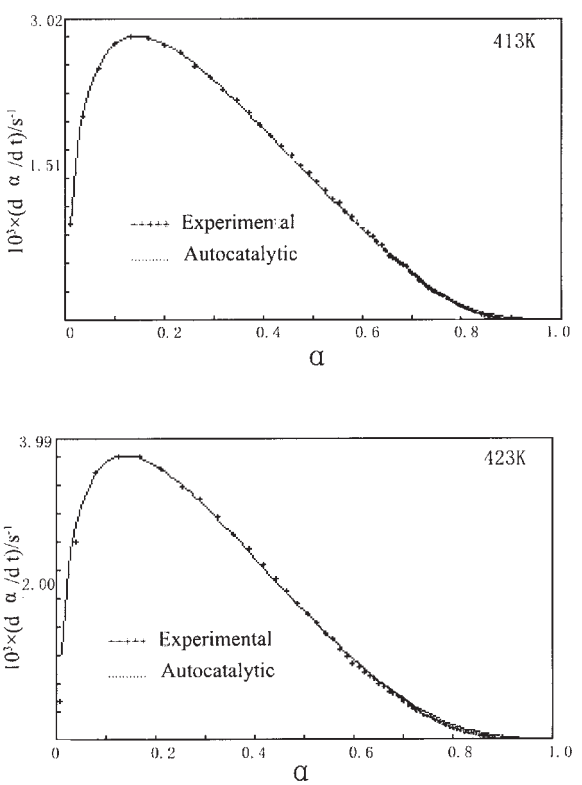

Figure 7 Comparison of the experimental data and theoretical values calculated with eq. (7): $d\alpha/dt$ versus α at 413 and 423 K

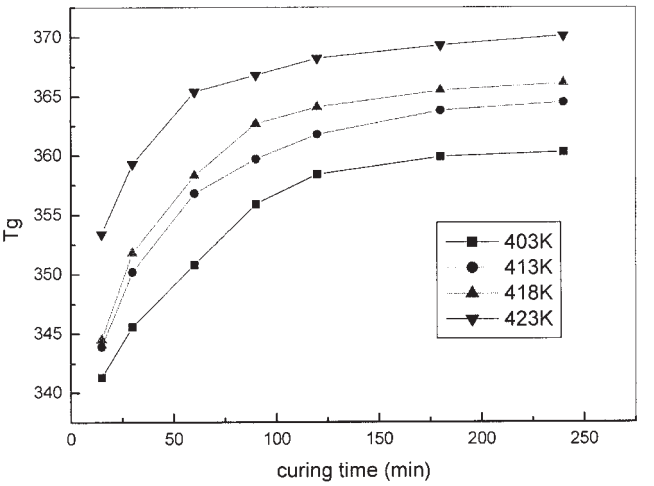

Figure 8 T_g values of *o*-CFER/DDE cured isothermally at different temperatures for various periods.

T_g and the curing process

T_g has been used directly as a parameter for conversion in the analysis of reaction kinetic models,[23,24] and there is a one-to-one relationship between T_g and the degree of cure. It is a convenient parameter because of the ease of measuring T_g by TBA, and it is particularly useful at high conversions and after vitrification because of the nonlinearity of T_g versus conversion reactions.[25,26] T_g's of *o*-CFER/DDE specimens cured isothermally at different temperatures for various periods of time obtained from TBA measurements are plotted versus the cure time in Figure 8. Different glass-transition behaviors occurred for the samples with different degrees of cure. T_g increased with the curing time and temperature.

At low T_c's, T_g increased during the early stages of cure and then leveled off and remained low in comparison with those at higher T_c's. Even if we prolonged the curing time at a low T_c, the resin system did not attain a high conversion. This result was different from that of the DSC experiment because the curing time was much longer than that for DSC. Because vitrification usually drastically lowers the reaction rate, a complete cure usually involves temperatures in the vicinity of the maximum of T_g. This is indicative of autocatalytic kinetics in the first stages and a diffusion-controlled reaction as T_g rises.[22] Similar results were obtained in our study of the conversion or reaction rate versus the time at different isothermal T_c's.

At the beginning of the curing reaction, the degree of cure was low, and the sample yielded a low T_g value. At this stage, the process was characterized by a gradual increase in the molecular weight, and this transition behavior reflected the movement of molecular chains in the system. Because only lower molecular chains existed and had a lower viscosity at this

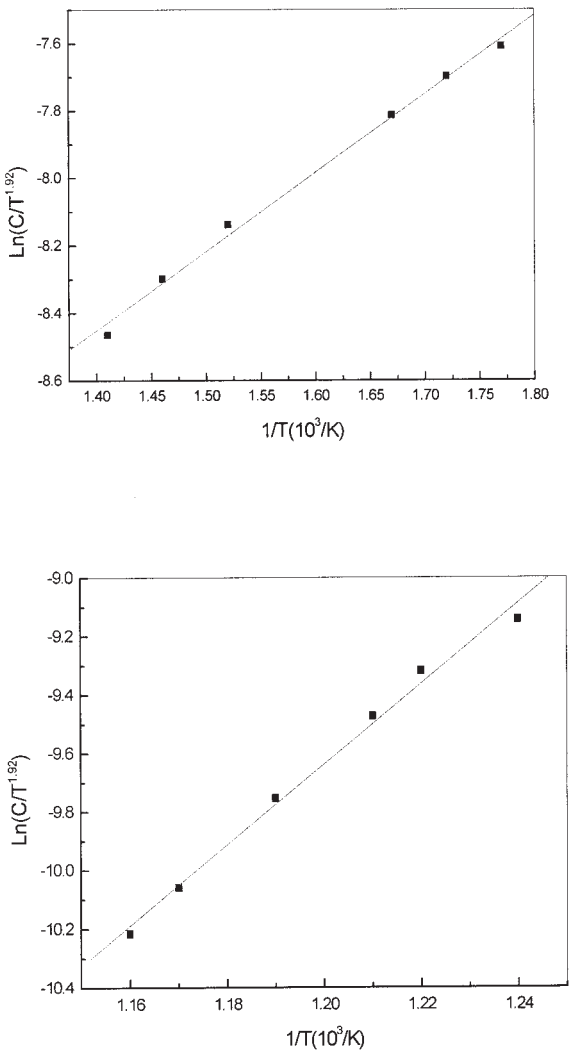

Figure 9 $\ln(C/T^{1.92})$ versus the reciprocal of the reaction temperature ($1/T$) for thermal degradation in the first and second steps.

stage, there were many chances for the molecules to collide, and this resulted in a high reaction rate. With the weight-average molecular weight increasing, most of the reactive functional groups were attached to the gel, and their mobilities were very limited, so the curing reaction became diffusion-controlled. The crosslinking density further increased with increasing reaction time, and T_g of the network was enhanced with a decrease in the distance between crosslink points. At this time, the sample was highly cured, and the T_g value became higher.

Thermal degradation

The weight-loss fractions of the resin were calculated, and the weight-loss rates are shown as a function of temperature in Figure 9. The TGA trace of DDE-cured *o*-CFER revealed two degradation steps in an air atmosphere. The following kinetic equation was assumed to hold true for the thermal degradation reaction:[10,11]

$$\ln(C/T^{1.92}) = \ln\frac{AE}{\phi R} + 3.77 - 1.92\ln E - \frac{E}{RT} \quad (8)$$

where C is equal to W/W_0, W is the remaining weight, W_0 is the total weight, E is the degradation activation energy, A is the frequency factor, ϕ is the heating rate, and R is the ideal gas constant. The degradation activation energy of the different stages was calculated from plots of the weight-loss function [$\ln(C/T^{1.92})$] versus the reciprocal of the reaction temperature. E_1 and E_2 were the degradation activation energies of the first and second stages, respectively. The activation energy of thermal degradation for the system in the first step was 19.42 kJ mol^{-1}, and the linear correlation coefficient was 0.9974. The second step was 128.14 kJ mol^{-1}, and the linear correlation coefficient was 0.9832. The degradation activation energy in the second stage was much higher than that in the first stage, and this showed that the breaking of strong bonds took place in the second stage, whereas weak bonds were broken in the first stage.

CONCLUSIONS

The cure reaction for the *o*-CFER/DDE system showed autocatalytic kinetic behavior in the kinetically controlled stage and was well described with the model proposed by Kamal,[5] which includes two rate constants, k_1 and k_2, and two reaction orders, m and n. The curing reaction during the later stage was practically diffusion-controlled. To consider the diffusion effect more precisely, we added $f(\alpha)$ to Kamal's equation to make it possible to describe and predict the cure reaction of this epoxy resin [eq. (6)]. The theoretical values agreed very well with the experimental data.

The curing process of *o*-CFER/DDE was different from that of bisphenol epoxy resin. A long curing time and a higher temperature were necessary to achieve a higher conversion and a higher T_g. The highest T_g was 370.1 K.

The TGA trace of this system revealed two decomposition stages and showed first-order degradation reaction kinetics. The activation energies of thermal degradation in the first and second stages were 19.42 and 128.14 kJ mol^{-1}, respectively.

References

1. Zhang, Z. F. Thermosetting Resin 1993, 8, 46.
2. Sun, Q. L.; Tian, X. H. Thermosetting Resin 1986, 1, 25.
3. Iwai; Akira; Saiki. Jpn. Kokai Tokkyo Koho 80,727 (2002).
4. Liu, S. G.; Liao, H. Thermosetting Resin 2001, 16, 38.

5. Kamal, M. R. Polym Eng Sci 1974, 14, 23.
6. Opalicki, M.; Kenny, J. M.; Nicolais, L. J Appl Polym Sci 1996, 61, 1025.
7. Khanna, U.; Chanda, M. J Appl Polym Sci 1993, 49, 319.
8. Duswalt, A. A. Thermochim Acta 1974, 8, 57.
9. Kenny, J. M.; Opalicki, M. Makromol Chem Macromol Symp 1993, 68, 41.
10. Liu, Z. H. Thermoanalysis Introduction; Chemical Industry: Beijing, 1991; p 100.
11. Madhusudanan, P. M.; Krishnan, K.; Ninan, K. N. Thermochim Acta 1986, 97, 189.
12. Ren, L. B. Thermosetting Resin 1998, 13, 17.
13. Jay, R. R. Anal Chem 1964, 36, 665.
14. Woo, E. M.; Seferis, J. C. J Appl Polym Sci 1990, 40, 1237.
15. Ghaemy, M.; Riahy, M. H. Eur Polym J 1996, 32, 1207.
16. Keenan, M. R. J Appl Polym Sci 1987, 33, 1725.
17. Barton, J. M. Adv Polym Sci 1985, 72, 111.
18. Ryan, M. E.; Dutta, A. Polymer 1979, 20, 203.
19. Moroni, A.; Mijiovic, J.; Pearce, E. M.; Foun, C. C. J Appl Polym Sci 1986, 32, 3761.
20. Kenny, J. M. J Appl Polym Sci 1994, 51, 761.
21. Cole, K. C.; Hechler, J. J.; Noel, D. Macromolecules 1991, 24, 3098.
22. Chern, C. S.; Poehlein, G. W. Polym Eng Sci 1987, 27, 782.
23. Simon, S. L.; Gillham, J. K. J Appl Polym Sci 1993, 47, 461.
24. Wisanrakkit, G.; Gillham, J. K. J Appl Polym Sci 1990, 41, 2885.
25. Venditti, R. A.; Gillham, J. K. J Appl Polym Sci 1997, 64, 3.
26. Wisanrakkit, G.; Gillham, J. K.; Enns, J. B. J Appl Polym Sci 1990, 41, 1895.